Heat and Mass Transfer 37 (2001) 403–408 © Springer-Verlag 2001

g-Jitter induced free convection near a stagnation point

D. A. S. Rees, I. Pop

Abstract The effect of a small but fluctuating gravitational field, characteristic of *g*-jitter, on the flow near the forward stagnation point of a two-dimensional symmetric body resulting from a step change in its surface temperature has been considered in this paper. The transformed equations are solved numerically by a very efficient finite-difference method known as the Keller-box technique to investigate the effects on the shear stress and rate of heat transfer of variations in the Prandtl number, Pr, the forcing amplitude, a, and the forcing frequency, ω. It has been found that these parameters affect considerably the shear stress and the rate of heat transfer.

List of symbols

a	magnitude of the sinusoidal gravity modulation
f	reduced stream function
g	time-dependent gravitational velocity
g_0	mean gravitational field
Gr	Grashof number
k	unit vector pointing vertically downward
ℓ	length scale
Pr	Prandtl number
$r(x)$	non-dimensional distance from the axis of the symmetric body to its surface
t	non-dimensional time
T	fluid temperature
T_w	wall temperature
T_∞	ambient temperature
u, v	non-dimensional velocity components along x and y axes
x, y	non-dimensional coordinates measured along the surface of the body and normal to it, respectively

Greek symbols

θ	non-dimensional temperature
Ψ	non-dimensional stream function
τ	reduced non-dimensional time
ω	frequency of the single-harmonic component of oscillation

Superscripts

–	dimensional variables
$'$	differentiation with respect to y

Received on 28 February 2000

D. A. S. Rees
Department of Mechanical Engineering, University of Bath
Claverton Down, Bath, BA2 7AY, UK

I. Pop
Faculty of Mathematics, University of Cluj, R-3400 Cluj
CP 253, Romania

1 Introduction

A well-understood problem in buoyancy-driven convection is the flow induced in a Boussinesq fluid by a heated body in the presence of a constant downward gravitational field. Recently, there has been a great deal of interest in the study of the effect of complex body forces on fluid motion. Such forces can arise in a number of ways, for example when a system with density gradients is subject to vibrations. The resulting buoyancy forces, which are produced by the interaction of density gradients with the acceleration field, have a complex spatio-temporal structure depending on both the nature of density gradients and the spatial and frequency distribution of the vibration-induced acceleration field. The effect of such forces on fluid motion is known as gravity modulation or *g*-jitter induced flow.

Numerous attempts have been made to estimate and calculate the effects of time varying *g*-jitter on the convective flow. Amin [1] has investigated the heat transfer from a sphere immersed in an infinite fluid medium in a zero-gravity environment under the influence of *g*-jitter. She has shown that heat transfer is negligibly small for high-frequency *g*-jitter but under special circumstances, when the Prandtl number is sufficiently high, low-frequency *g*-jitter may play an important role. There have also been a number of studies to investigate the effects of *g*-jitter on fluid motion of a viscous fluid in cavities and channels, e.g. Biringen and Peltier [2], Biringen and Danabasoglu [3], Alexander et al. [4], Farooq and Homsy [5, 6], Li [7], Pan and Li [8], and Suresh et al. [9]. These studies have shed some light on the basic nature of *g*-jitter effects and have provided a thrust to devise useful mechanisms by which the *g*-jitter induced convective flows may be suppressed. Also a fundamental understanding of some isolated aspects of fluid dynamic systems in an unsteady gravitational environment has been given. Given that perturbative accelerations exist in the microgravity environment, an estimation of the critical frequency ranges that drives a significant amount of convective motion, critical directions of modulation, and the effects of random forcing have been estimated. On the other hand, the above mentioned papers have been motivated by the need to model fluid processes under microgravity conditions on board spacecraft (see, Alexander [10]). Under these con-

ditions, arbitrarily oriented gravitational fluctuations give rise to body forces and affect flows that would otherwise be steady. It has been shown that such time-dependent forces can significantly affect the stability of the system. Further, in the space lab and Shuttle environments, the existence of perturbative accelerations, characterized by a broad frequency spectrum, is well known. These perturbations are caused by mechanical vibrations, Orbiter maneuvers, and crew activities and cannot be totally eliminated from the space manufacturing environment. These studies have shed some light on the basic nature of g-jitter effects and have provided a thrust to devise useful mechanisms by which the g-jitter induced convective flows may be suppressed. An extensive overview of these and other sources of unsteady gravitational accelerations, derived from estimates based on measurements in the spacelab engineering model, has been documented in the paper by Gresho and Sani [11]. Accordingly, peak accelerations of $2.6 \times 10^{-2} g$ (g is the terrestrial acceleration) due to crew activities are expected. Such undesirable perturbations during manufacturing processes affect heat and mass transfer and may have detrimental effects on the quality of material processed in space (see Biringen and Danabasoglu [3]). This situation could be especially important in space-based crystal growth where the elimination/reduction of natural convection is essential to the quality of the crystals.

In this paper, we intend to study the behavior of g-jitter induced free convection flow of a viscous and incompressible fluid near the forward stagnation point of a two-dimensional symmetric body resulting from a step change in its surface temperature. We consider a simple model problem in which the gravitational field takes the form

$$\mathbf{g} = g_0[1 + a\cos(\pi\omega t)]\mathbf{k} \tag{1}$$

where g_0 is the time-averaged value of $\mathbf{g}$ acting along the direction of the unit vector $\mathbf{k}$, a is a scaling parameter which gives the magnitude of the sinusoidal gravity modulation relative to g_0, t is the time and ω is the frequency of the single-harmonic component of oscillation. We notice that the case of a constant downward gravitational field has been the subject of several numerical and analytical treatments, e.g. Ingham et al. [12], Sano and Wakitani [13], Chaudhary and Merkin [14] and Slaouti et al. [15]. There are also two recent papers by Rees and Pop [16, 17] on g-jitter effects on the free convection flow in a porous medium.

2 Basic equations

Consider the unsteady free convection boundary-layer around a two-dimensional symmetric body immersed in a viscous and incompressible Boussinesq fluid, which is at a uniform temperature T_∞. It is assumed that at time $t = 0$, the temperature of the body surface is suddenly increased to the constant value T_w, where $T_w > T_\infty$. We also assume that a time-dependent body force in accordance with Eq. (1) acts on the fluid and, as a result of volume expansion, fluid motion will exist. Under the usual boundary-layer and Boussinesq approximations, the governing equations in non-dimensional form can be written as

$$\frac{\partial u}{\partial x} + \frac{\partial v}{\partial y} = 0 \tag{2}$$

$$\frac{\partial u}{\partial t} + u\frac{\partial u}{\partial x} + v\frac{\partial u}{\partial y} = \frac{\partial^2 u}{\partial y^2} + \left[1 - \left(\frac{\mathrm{d}r}{\mathrm{d}x}\right)^2\right]^{1/2} \times [1 + a\cos(\pi\omega t)]\theta \tag{3}$$

$$\frac{\partial \theta}{\partial t} + u\frac{\partial \theta}{\partial x} + v\frac{\partial \theta}{\partial y} = \frac{1}{\mathrm{Pr}}\frac{\partial^2 \theta}{\partial y^2} \tag{4}$$

where the non-dimensional variables are defined as

$$t = \mathrm{Gr}^{1/2}(\nu/\ell^2)\bar{t}, \quad (x, r) = (\bar{x}, \bar{r})/\ell, \quad y = \mathrm{Gr}^{1/4}(\bar{y}/\ell)$$
$$u = \mathrm{Gr}^{-1/2}(\ell/\nu)\bar{u}, \quad v = \mathrm{Gr}^{-1/4}(\ell/\nu)\bar{v}$$
$$\theta = (T - T_\infty)/(T_w - T_\infty), \quad \omega = \mathrm{Gr}^{-1/2}(\ell^2/\nu)\bar{\omega} \tag{5}$$

Here $\bar{x}$ and $\bar{y}$ are the Cartesian coordinates measured along the surface of the body and normal to it, respectively, $\bar{u}$, and $\bar{v}$ are the velocity components along $\bar{x}$- and $\bar{y}$-directions, $\bar{r}(\bar{x})$ is the distance from the axis of the symmetric body to its surface, ℓ is a length scale, and Pr and Gr are the usual Prandtl and Grashof numbers.

Nearly the forward stagnation point of the body, the radius $r(x)$ is given by

$$r(x) \approx x - \frac{1}{6}x^3 + O(x^5) \tag{6}$$

and hence

$$\left[1 - \left(\frac{\mathrm{d}r}{\mathrm{d}x}\right)^2\right]^{1/2} \approx x + O(x^3) \tag{7}$$

Thus, Eqs. (2)–(4) have the semi-similar solution of the form

$$\Psi = xf(y, t), \quad \theta = \theta(y, t) \tag{8}$$

where Ψ is the stream function which is defined in the usual way as $u = \partial\Psi/\partial y$ and $v = -\partial\Psi/\partial x$. On using (8) in Eqs. (3) and (4), we get

$$f''' + ff'' - (f')^2 + [1 + a\cos(\pi\omega t)]\theta = \frac{\partial f'}{\partial t} \tag{9}$$

$$\frac{1}{\mathrm{Pr}}\theta'' + f\theta' = \frac{\partial \theta}{\partial t} \tag{10}$$

which are subject to the initial and boundary conditions

$$\begin{aligned} t = 0: &\quad f = \theta = 0 && \text{for any } y \\ t > 0: &\quad f = f' = 0,\ \theta = 1 && \text{on } y = 0 \\ &\quad f' \to 0,\ \theta \to 0 && \text{as } y \to \infty \end{aligned} \tag{11}$$

We find it more convenient to rescale t by writing $\tau = \omega t$, so that Eqs. (9) and (10) become

$$f''' + ff'' - (f')^2 + [1 + a\cos(\pi\tau)]\theta = \omega\frac{\partial f'}{\partial \tau} \tag{12}$$

$$\frac{1}{\mathrm{Pr}}\theta'' + f\theta' = \omega\frac{\partial\theta}{\partial\tau} \tag{13}$$

with the initial and boundary conditions as given by (11).

3 Results and discussion

Equations (12) and (13) subject to the boundary conditions (11) were solved numerically using the well-known Keller-box method first introduced in Keller and Cebeci [18] (see also Cebeci and Bradshaw [19]). In this numerical scheme the equations were reduced to first order form in y and discretised using central differences in both y and τ directions. The resulting nonlinear set of difference equations were solved using a straightforward multidimensional Newton–Raphson iteration scheme. Our detailed results are given for $\mathrm{Pr} = 6.7, 0.7$ and 0.01 and these values represent water, air and liquid metals; in the first two cases we used a uniform grid in the y direction consisting of 201 points in the range $0 \le y \le 10$, whereas for the third case, where the boundary layer is considerably thicker, we used a nonuniform grid of 82 points lying in the range $0 \le y \le 100$ where intervals formed a geometric progression. The computations were always started with the appropriate steady solution to the $a = 0$ case and convergence to a steady periodic state was demanded to have taken place when

$$\max_{\tau} |\theta'(0,\tau) - \theta'(0,\tau-2)| < 10^{-6} \tag{14}$$

over a whole period. In general convergence occurs very rapidly for relatively large values of ω, but in all the cases considered convergence occurred in fewer than 100 periods. The results we present are concerned with the converged state, rather than on the transient approach to periodic flow.

Our numerical results are summarised in Tables 1 and 2 and in Figs. 1–4 which show how the surface rate of heat transfer, $\theta'(0,\tau)$, and shear stress, $f''(0,\tau)$, over one period are affected by different values of the Prandtl number, Pr, the forcing frequency, ω, and the forcing amplitude, a. Figures 1–3 correspond to $\mathrm{Pr} = 0.7, 6.7$ and 0.01, respectively. In these figures we vary a from 0 to 1 and use three different values of ω: 0.2, 1 and 5. We do not allow a to take values above 1 since this is equivalent to having the perceived gravity reverse its direction over part of the g-jitter cycle.

Table 1. Values of the mean heat transfer rate, $\Theta'(0)$, and the mean shear stress, $F''(0)$, for Pr = 6.7

a	$\Theta'(0)$			$F''(0)$		
	$\omega = 0.2$	$\omega = 1$	$\omega = 5$	$\omega = 0.2$	$\omega = 1$	$\omega = 5$
0.000	0.78245	0.78245	0.78245	0.58945	0.58945	0.58945
0.100	0.78200	0.78241	0.78247	0.58926	0.58905	0.58912
0.200	0.78121	0.78233	0.78246	0.58885	0.58861	0.58880
0.300	0.78006	0.78220	0.78245	0.58821	0.58815	0.58848
0.400	0.77856	0.78203	0.78244	0.58734	0.58764	0.58815
0.500	0.77668	0.78181	0.78242	0.58623	0.58711	0.58781
0.600	0.77443	0.78156	0.78240	0.58490	0.58654	0.58747
0.700	0.77178	0.78126	0.78238	0.58334	0.58594	0.58712
0.800	0.76871	0.78092	0.78235	0.58154	0.58530	0.58677
0.900	0.76519	0.78053	0.78233	0.57952	0.58463	0.58641
1.000	0.76119	0.78011	0.78229	0.57727	0.58392	0.58605

Table 2. Values of the mean heat transfer rate, $\Theta'(0)$, and the mean shear stress, $F''(0)$, for Pr = 0.7

a	$\Theta'(0)$			$F''(0)$		
	$\omega = 0.2$	$\omega = 1$	$\omega = 5$	$\omega = 0.2$	$\omega = 1$	$\omega = 5$
0.000	0.37023	0.37023	0.37023	0.85935	0.85935	0.85935
0.100	0.36995	0.37018	0.37024	0.85886	0.85867	0.85895
0.200	0.36938	0.37010	0.37023	0.85774	0.85787	0.85855
0.300	0.36852	0.36997	0.37022	0.85598	0.85694	0.85815
0.400	0.36735	0.36981	0.37021	0.85356	0.85589	0.85773
0.500	0.36586	0.36960	0.37020	0.85047	0.85470	0.85730
0.600	0.36400	0.36935	0.37019	0.84667	0.85339	0.85686
0.700	0.36174	0.36907	0.37018	0.84211	0.85195	0.85640
0.800	0.35902	0.36874	0.37016	0.83675	0.85038	0.85594
0.900	0.35576	0.36837	0.37014	0.83053	0.84868	0.85546
1.000	0.35186	0.36796	0.37012	0.82334	0.84684	0.85497

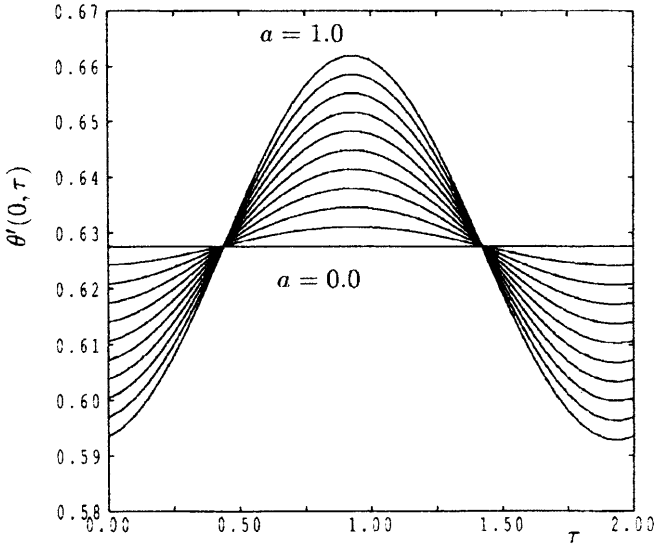

Fig. 1. The rate of heat transfer, $\theta'(0,\tau)$, for $\omega = 5$ with $a = 0.0, 0.1, \ldots, 1.0$. The solutions represent the periodic flow after the decay of transients

When $\omega = 5$ in Fig. 1, the effect of increasing a is to give an almost proportional increase in the local shear stress response. The peak in the acceleration felt by the system occurs at $\tau = 0.5$ in this figure but the peak in the response occurs after this. Inspection of the $\omega = 1$ and $\omega = 0.2$ cases shows a similar behavior although the peak response occurs closer to the time of peak acceleration as ω decreases. The corresponding curves for the surface rate of heat transfer, $\theta'(0,\tau)$, show exactly the same trends although the phase lag is much greater in all cases. Indeed, for $\omega = 5$, the peak response is almost exactly half a cycle behind that of the perceived acceleration. As with the surface shear stress, $f''(0,\tau)$, the variation in the phase of the peak response as a changes is imperceptible. For larger values of ω, $\partial\theta/\partial\tau$ is quite small, see Eqs. (12) and (13), and therefore we would expect the response to lag quite

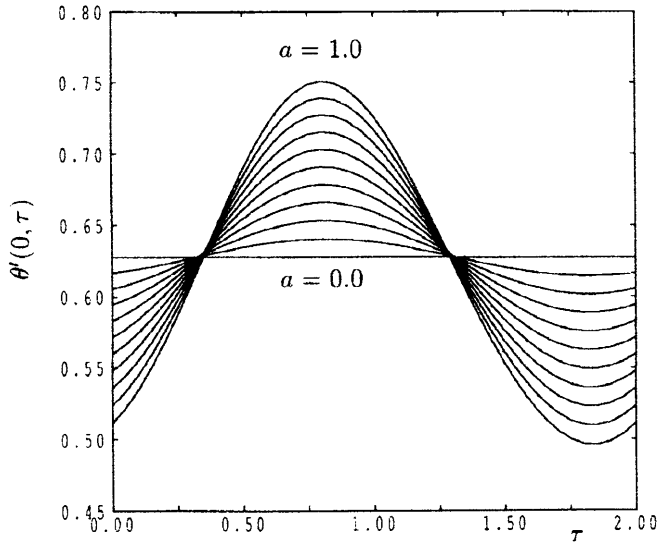

Fig. 2. The rate of heat transfer, $\theta'(0,\tau)$, for $\omega = 1$ with $a = 0.0, 0.1, \ldots, 1.0$. The solutions represent the periodic flow after the decay of transients

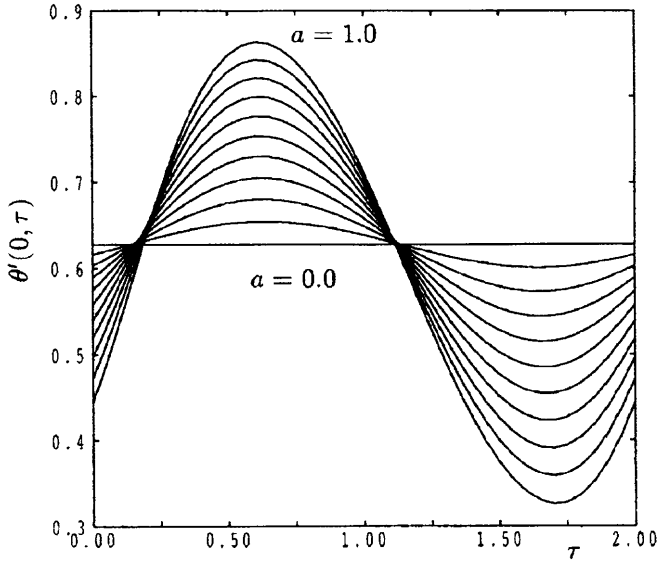

Fig. 3. The rate of heat transfer, $\theta'(0,\tau)$, for $\omega = 0.2$ with $a = 0.0, 0.1, \ldots, 1.0$. The solutions represent the periodic flow after the decay of transients

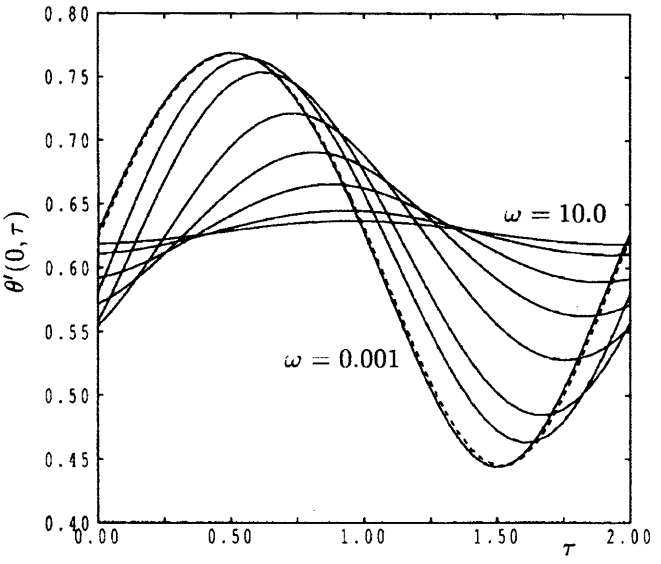

Fig. 4. The rate of heat transfer, $\theta'(0,\tau)$, for $a = 0.5$ with $\omega = 0.001, 0.01, 0.1, 0.2, 0.5, 1.0, 2.0, 5.0$ and 10.0. The solution for $\omega = 0.01$ is displayed as a dashed line. The solutions represent the periodic flow after the decay of transients

Table 3. Values of the mean heat transfer rate, $\Theta'(0)$, and the mean shear stress, $F''(0)$, for Pr = 0.01

a	$\Theta'(0)$			$F''(0)$		
	$\omega = 0.2$	$\omega = 1$	$\omega = 5$	$\omega = 0.2$	$\omega = 1$	$\omega = 5$
0.000	0.10873	0.10873	0.10873	1.10678	1.10678	1.10678
0.100	0.10872	0.10872	0.10873	1.10591	1.10583	1.10635
0.200	0.10870	0.10871	0.10873	1.10410	1.10454	1.10590
0.300	0.10867	0.10869	0.10873	1.10130	1.10291	1.10542
0.400	0.10863	0.10867	0.10873	1.09749	1.10094	1.10492
0.500	0.10857	0.10864	0.10873	1.09259	1.09861	1.10440
0.600	0.10849	0.10861	0.10872	1.08653	1.09594	1.10386
0.700	0.10840	0.10858	0.10872	1.07917	1.09292	1.10330
0.800	0.10829	0.10854	0.10872	1.07034	1.08955	1.10271
0.900	0.10816	0.10849	0.10872	1.05979	1.08581	1.10210
1.000	0.10798	0.10844	0.10872	1.04717	1.08172	1.10147

substantially behind that of the perceived gravitational acceleration, and conversely for small values of ω.

In Fig. 2 we display the corresponding curves for Pr = 0.7, a lower value than that in Fig. 1. The main difference between Figs. 1 and 2 lies in the range of values that $\theta'(0,\tau)$ and $f''(0,\tau)$ take; this is clearly related to the value of Pr. For when Pr decreases, the thermal conductivity increases in importance relative to the viscosity, and conduction occurs more easily than advection. Therefore, the thermal boundary-layer increases in thickness as Pr decreases, and this is the cause in the decreased overall value of the surface rate of heat transfer. This trend may be seen by comparing corresponding rate of heat transfer curves between Figs. 2 and 3, where the latter assumes that Pr = 0.01.

The influence of changes in ω may be seen by comparing Figs. 1–3. But in Fig. 4 we show more directly how the value of ω influences the time-periodic flow obtained. Here we choose $a = 0.5$ and use the same values of Pr as above, but we also use a wider range of values of ω than is used in Figs. 1–3. The changes in the peak response in both $\theta'(0,\tau)$ and $f''(0,\tau)$ are now seen very clearly. At low values of ω the response is quasi-static and the whole flow and temperature field is determined at leading order by the size of the perceived gravitational acceleration at any point in time. But as ω increases, the peak response is delayed progressively and the amplitude of the variation of the response over a period also decreases. This latter effect is stronger for the shear stress than for the rate of heat transfer. Indeed, the rate of heat transfer is almost constant when $\omega > 10$.

Table 4. Values of the mean heat transfer rate, $\Theta'(0)$, and the mean shear stress, $F''(0)$, for $a = 0.5$

ω	$\Theta'(0)$			$F''(0)$		
	Pr = 6.7	Pr = 0.7	Pr = 0.01	Pr = 6.7	Pr = 0.7	Pr = 0.01
0.001	0.77252	0.36555	0.10858	0.58224	0.84882	1.09364
0.010	0.77256	0.36559	0.10858	0.58245	0.84902	1.09380
0.100	0.77338	0.36533	0.10857	0.58455	0.84956	1.09303
0.200	0.77668	0.36586	0.10857	0.58623	0.85047	1.09259
0.500	0.78072	0.36829	0.10858	0.58706	0.85290	1.09424
1.000	0.78181	0.36960	1.10864	0.58711	0.85470	1.09861
2.000	0.78223	0.37005	0.10870	0.58734	0.85608	1.10216
5.000	0.78242	0.37020	0.10873	0.58781	0.85730	1.10440
10.000	0.78249	0.37024	0.10873	0.58816	0.85787	1.10521

Although the flow and temperature fields vary widely in the presence of *g*-jitter, it is important to determine how the mean shear stress, $F''(0)$, and rate of heat transfer, $\Theta'(0)$, vary with changes in the amplitude and frequency of the *g*-jitter effect. To this end we have used the solutions shown in Figs. 1–4 and integrated them numerically over one period using the trapezoidal rule to obtain their respective means. These means are displayed in Tables 1–4, where the first three tables correspond to $\mathrm{Pr} = 6.7, 0.7$ and 0.01, respectively, while Table 4 gives mean values of $a = 0.5$.

There are very clear differences between the first three Tables due to the different values of Pr, but within each table we see that the overall effect of even very large *g*-jitter amplitudes is fairly small. For instance, for $\mathrm{Pr} = 6.7$, the mean rate of heat transfer varies by less than 3% when a varies from 0 to 1 for $\omega = 0.2$. The corresponding decreases for other values of ω and for the surface shear stress are smaller than this. The corresponding maximum changes in the surface rate of heat transfer for $\mathrm{Pr} = 0.7$ and 0.01 are 5% and 7%, respectively.

When $a = 0.5$, as given in Table 4, the variation in the mean surface rate of heat transfer is very small indeed as ω varies from quasi-static values (0.001) to very fast variations ($\omega = 10$). And again, small values of the Prandtl number yield very small variations with ω. For both the rate of heat transfer and the surface shear stress increasing values of ω corresponds generally to increasing mean values.

4 Conclusions

In this paper we have investigated the effect of sinusoidal gravity modulation of size a on the unsteady free convection flow near the forward stagnation point of a two-dimensional symmetric body resulting from a step change in its surface temperature. We have theoretically examined the effects of the forcing amplitude, a, and the forcing frequency, ω, for three values of the Prandtl number $\mathrm{Pr} = 0.01$, 0.7 and 6.7. A detailed numerical solution of the governing equations showed that so long as the value of Pr was kept constant, the effect of increasing of the values of a is to give an almost proportional increase in the shear stress and rate of heat transfer responses. However, the phase lag is much greater in all cases as can be seen in Figs. 1–3. As shown in these figures, *g*-jitter induced flow decreases the peak of the shear stress and increases the peak of the rate of heat transfer as ω increases. Further, it was found that at a fixed value of $a = 0.5$ (say) and at low values of ω, the response in the shear stress and surface rate of heat transfer is quasi-static and the whole flow and temperature field is determined at leading order by the size of the perceived gravitational acceleration at any point in time. It was also shown that for a low Prandtl number and some values of ω, the shear stress becomes more excitable than the rate of heat transfer (see Fig. 4). The gravitational modulation is more effective in investigating a transition from conductive to a convective temperature field at higher frequencies.

Finally, we mention that the persistance of the velocity and temperature oscillations even when the thermal field is conductive, could be of importance in mass transport processes in the presence of impurities.

References

1. **Amin N** (1988) The effect of g-jitter on heat transfer. Proc R Soc London A 419: 151–172
2. **Biringen S; Peltier LJ** (1990) Computational study of 3-D Benard convection with gravitational modulation. Phys Fluids A 2: 279–283
3. **Biringen S; Danabasoglu G** (1990) Computation of convective flow with gravity modulation in rectangular cavities. AIAA J Thermophys Heat Transfer 4: 357–365
4. **Alexander JID; Amirondine S; Ouzzani J; Rosenberger F** (1991) Analysis of the low gravity tolerance of Bridgman–Stockbarger crystal growth II. Transient and periodic acceleration. J Cryst Growth 113: 21–38
5. **Farooq A; Homsy GM** (1994) Streaming flows due to g-jitter-induced natural convection. J Fluid Mech 271: 351–378
6. **Farooq A; Homsy GM** (1996) Linear and nonlinear dynamics of a differentially heated slot under gravity modulation. J Fluid Mech 313: 1–38
7. **Li BO** (1996) g-Jitter induced free convection in a transverse magnetic field. Int J Heat Mass Transfer 39: 2853–2890
8. **Pan B; Li BO** (1998) Effect of magnetic fields on oscillating mixed convection. Int J Heat Mass Transfer 41: 2705–2710
9. **Suresh VA; Christov CI; Homsy GM** (1999) Resonant thermocapillary and buoyant flows with finite frequency gravity modulation. Phys Fluids 11: 2585–2576
10. **Alexander JID** (1990) Low gravity experiment sensitivity to residual acceleration: A review. Microgravity Sci Technol III 2: 52–68
11. **Gresho PM; Sani RL** (1970) The effects of gravity modulation on the stability of a heated fluid layer. J Fluid Mech 40: 783–806
12. **Ingham DB; Merkin JH; Pop I** (1984) Unsteady free convection of a stagnation point of attachment on an isothermal surface. Int J Math and Math Sci 7: 599–614
13. **Sano T; Wakitani S** (1984) Unsteady free convection near a forward stagnation point at small Prandtl numbers. J Phys Soc Japan 53: 1277–1283
14. **Chaudhary MA; Merkin JH** (1996) Free convection stagnation-point boundary layers driven by catalytic surface reactions: II Times to ignition. J Engng Math 30: 403–415
15. **Slaouti A; Takhar HS; Nath G** (1998) Unsteady free convection flow in the stagnation-point region of a three dimensional body. Int J Heat Mass Transfer 41: 3397–3408

16. **Rees DAS; Pop I** (2000) The effect of g-jitter on vertical free convection boundary-layer in a porous medium. Int Comm Heat Mass Transfer 27: 415–424
17. **Rees DAS; Pop I** (2001) The effect of g-jitter on free convection near a stagnation point in a porous medium. Int J Heat Mass Transfer 44: 877–883
18. **Keller HB; Cebeci T** (1971) Accurate numerical methods in boundary-layer flows. I. Two-dimensional laminar flows. In: Holt M (ed.) Second Int Conf on Numerical Methods in Fluid Dynamics, Springer, New York, pp. 92–100
19. **Cebeci T; Bradshaw P** (1984) Physical and Computational Aspects of Convective Heat Transfer. Springer, New York